
Proceedings Paper:
Bugryniec, P., Davidson, J. orcid.org/0000-0002-6576-3995 and Brown, S. orcid.org/0000-0001-8229-8004 (2020) Computational modelling of thermal runaway propagation potential in lithium iron phosphate battery packs. In: Cruden, A., (ed.) Energy Reports. 4th Annual CDT Conference in Energy Storage & Its Applications, 09-10 Jul 2019, Southampton, UK. Elsevier , pp. 189-197.

https://doi.org/10.1016/j.egyr.2020.03.024

Available online at www.sciencedirect.com
ScienceDirect
Energy Reports 6 (2020) 189–197
www.elsevier.com/locate/egyr

4th Annual CDT Conference in Energy Storage and Its Applications, Professor Andrew Cruden, 2019, 07–19, University of Southampton, U.K.

Computational modelling of thermal runaway propagation potential in lithium iron phosphate battery packs

Peter J. Bugryniec[a], Jonathan N. Davidson[b], Solomon F. Brown[a,*]

[a] *Department of Chemical & Biological Engineering, University of Sheffield, Sheffield, S1 3JD, United Kingdom of Great Britain and Northern Ireland*

[b] *Department of Electronic & Electrical Engineering, University of Sheffield, Sheffield, S1 4DE, United Kingdom of Great Britain and Northern Ireland*

Received 20 February 2020; accepted 22 March 2020

Abstract

It is widely accepted that Lithium-Iron Phosphate (LFP) cathodes are the safest chemistry for Li-ion cells, however the study of them assembled in to battery modules or packs is lacking. Hence, this work provides the first computational study investigating the potential of thermal runaway propagation (TRP) in packs constructed of LFP 18650 cells. Utilizing a 2D model of a battery pack in which one cell is assumed to experience an internal short circuit, it is found that TRP does not occur even under extreme environmental conditions. This shows the potential that LFP cells have at enabling safe and abuse resilient large scale batteries.

Peer-review under responsibility of the scientific committee of the 4th Annual CDT Conference in Energy Storage and Its Applications, Professor Andrew Cruden, 2019.

Keywords: Thermal runaway; Lithium-ion batteries; Battery safety; Battery hazards

1. Introduction

Lithium-ion batteries (LIBs) are widely used due to their superior performance over other battery chemistries [1,2]. However, LIBs do present a significant safety concern as they have the potential to go into catastrophic and hazardous failure through a process known as thermal runaway (TR) [3–5], depicted in Fig. 1.

Further, when cells are assembled into modules and packs the potential hazards are more severe, as the TR of a single cell presents a serious hazard to the surrounding cells [6,7], as the heat released by a single cell can dissipate to the neighbouring cells, which can in turn lead to these surrounding cells to heat up to the point that they themselves go into TR. Thus, this can be the start of a chain reaction of TR from cell-to-cell occurring throughout the entire module, known as thermal runaway propagation (TRP) [8].

* Corresponding author.
E-mail address: s.f.brown@sheffield.ac.uk (S.F. Brown).

https://doi.org/10.1016/j.egyr.2020.03.024

Peer-review under responsibility of the scientific committee of the 4th Annual CDT Conference in Energy Storage and Its Applications, Professor Andrew Cruden, 2019.

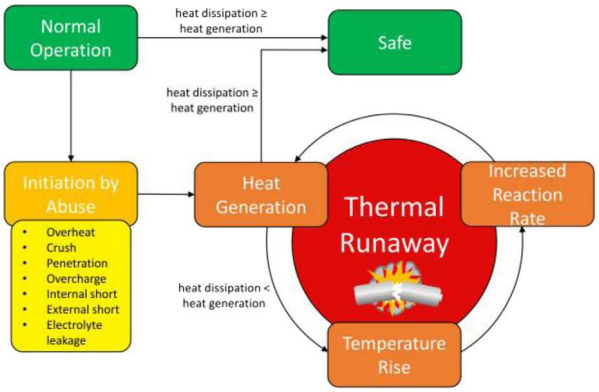

Fig. 1. Thermal runaway process within a single cell.

The severity of TR is, in part, a property of li-ion cell chemistry. With regards to this, LFP is reported to be the safest cathode composition for LIBs [9]. Even so, LFP batteries, including those in EV buses, have been reported to undergo TR [10–13]. Hence, it is important to develop the current limited research on LFP cell safety. As, to the authors' knowledge, only one study has been carried out on LFP packs, in which a module of pouch cells is studied [14]. Evidently, there is a need to expand the understanding of the TR behaviour of LFP packs when abused, to facilitate its wider adoption.

TR models for Li-ion cells have been developed by several authors, for different chemistries, based on describing the heat generated (by the decomposition of the cell) through Arrhenius equations, relating the reaction rate to temperature [15–22]. The determination of TRP or potential propagation of non LFP packs has been most accurately studied computationally by modelling the decomposition reactions in all cells, allowing for the propagation path and severity to be quantified [23–28].

The initiation of TR is typically done by simulating an internal short, modelled by an initial high temperature [23,24,26], or by modelling a percentage of the cell electrochemical energy been released over a prescribed time i.e. 10 s in a specified volume [25,27].

0D [27], 2D [26,29–31] and 3D [23,24,28,32,33] have all been utilized in modelling propagation. Typically, with regards to cylindrical cells, 2D geometry can be utilized to simplify relative long cylindrical cells. This is done in cases were the cells are arranged radially and when electrical connections are not considered (i.e. tabs) or other heating/cooling along the axis is not considered. 3D modelling provides the ability to model these assumptions. With regards to the inclusion of tabs, it has been shown that they are a significant heat transfer path, and can mean the difference between predicting a safe out come if not considered and predicting an unsafe, TRP, outcome if considered [26].

TRP is more likely to occur when a cell initiated into TR is in contact with the least number of neighbouring cells, and also when these neighbouring cells are also in the least contact with other cells [23,26]. Additionally, cells packed closer together lead to greater TRP severity. Electrical connections are important for both heat and charge transfer, while cells connected in parallel can experience Joule heating in a failed cell [7].

The time to failure of subsequent cells in TRP reduces due to the preheating from the previous cells undergoing TR [28]. Gas venting is shown to be a significant heat transfer mechanism, especially if it ignites and if the cells are contained within a rigid air tight casing, which also leads to TRP sooner [28,34].

Here, the aim is to investigate the TRP potential of battery packs constructed of 18650 LFP cells. First, a heuristic parameter estimation technique is used to develop a TR model in 1D, based on the classic 4 reaction system, of a single LFP cell. From this, a 2D model of an LFP 18650 cell is built, compared to the 1D model and validated against experimental data. Finally, a small 3-by-3 battery pack, modelled in 2D, is investigated under several initiation criteria and environmental criteria. The results of which are discussed in terms of TRP potential and suitability of LFP cells for packs of larger sizes.

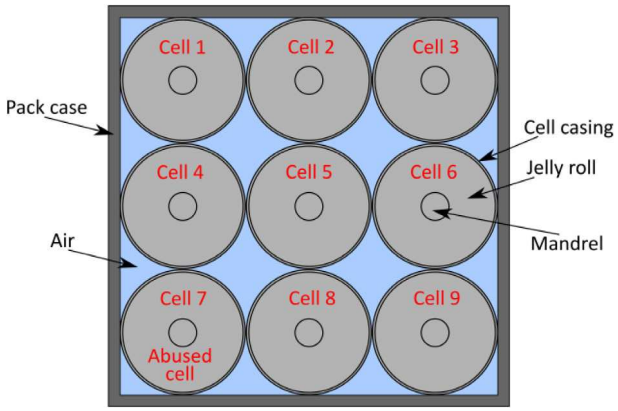

Fig. 2. Schematic of simulated geometry.

2. Methodology

To study the potential of TRP in LFP battery packs, a pack containing 9 cylindrical 18650 (LFP 1.5Ah 3.2V) cells (arranged in a 3-by-3 matrix) is considered as a case study, and represented by a 2D planar geometry. A schematic of the simulated geometry is presented in Fig. 2, while the dimensions of the pack components are given in Table 1.

The model is built in *COMSOL Multiphysics 5.2a* [35], in which the *Heat Transfer module* is used to implement the governing equations of conduction, convection and radiation. The model considers heat transfer by conduction within the cells, the pack case and the air surrounding the cells. Surface-to-surface radiation between the cells and the internal surface of the pack case is also considered, along with radiation from the outer surface of the pack case to the environment. The outer surface of the pack case is also subject to heat transfer by convection with a fixed heat transfer coefficient, while convection of the air in the pack is ignored.

Although 18650 cells are not symmetric along their length, due to the end cap at the positive terminal, the high thermal conductivity along the cells length allows the 2D planar assumption to be acceptable [36]. Electrochemical reactions, electrical connections between the cells and current flow between cells (which can occur when cells in parallel fail) are not considered. Further, gas venting and heat transfer by the flow of gases or their combustion is also not considered.

The geometry of each individual cell is represented by a mandrel, jelly roll and cell casing, see Fig. 2. Although the cells are represented by these three major domains, the cells are modelled as homogeneous material with average properties. The density and heat capacity values are equal to the average values calculated by Bugryniec et al. (2019), while average the radial thermal conductivity is estimated within literature values. These properties, and other thermo-physical and heat transfer properties, including those describing the air and the pack case (assumed to be acrylic plastic) are presented in Table 1. The construction of the cell domains in this manner is so that the volume specific heat generation by the decomposition of the jelly roll materials is only applied over the jelly roll region, thus leading to a more accurate calculation of overall heat generation.

The governing equations for the SEI, NE, PE and electrolyte decomposition reactions and the resulting heat generation used within this work follow those outlined by Refs. [15,17], and hence are not presented here.

The values of the parameters describing the decomposition reactions are determined through heuristic parameter estimation techniques and presented in Table 1. The parameter estimation was carried out through the comparison of simulations of a single cell under oven exposure to experimental data from Bugryniec et al. (2019) of the same test [37]. The resulting oven test simulation (in 2D) compared to the experimental data for a single cell is presented in Fig. 3. As the figure shows, while the abuse model does not predict features such as venting, time to peak temperature and post TR heat generation well, the model does predict severity very well. Hence, the model is applicable for preliminary investigation of LFP pack hazards.

Table 1. Model parameters.

Parameter (units)	Value	Parameter (units)	Value
Cell radius, r_{cell} (mm)	9	Frequency factor PE, A_{pe} (1/s)	2.000E08
Mandrel radius, r_{man} (mm)	2	Frequency factor electrolyte, A_e (1/s)	5.140E25
Cell case thickness, d_{can} (mm)	0.3	Heat of reaction SEI, H_{sei} (J/kg)	5.780E05
Cell height, h_{cell} (mm)	65	Heat of reaction NE, H_{ne} (J/kg)	3.428E06
Pack case thickness, d_{pack} (mm)	2	Heat of reaction PE, H_{pe} (J/kg)	2.414E05
Average heat capacity of cell, $C_{p,cell}$ (J/kg K)[d]	1005	Heat of reaction electrolyte, H_e (J/kg)	3.410E05
Average density of cell, ρ_{cell} (kg/m^3)[d]	2418	Reaction species initial value SEI, $C_{sei,0}(1)$[c]	0.15
Radial thermal conductivity of cell, κ_r (W/m K)[a]	0.5	Reaction species initial value NE, $C_{ne,0}(1)$[c]	0.75
Heat capacity of pack casing, $C_{p,pack\_casing}$ (J/kg K)[b]	1470	SEI layer thickness initial value, $t_{sei,0}(1)$[c]	0.033
Density of pack casing, ρ_{pack_casing} (kg/m^3)[b]	1190	Reaction species initial value PE, $C_{pe,0}(1)$[c]	0.04
Thermal conductivity of pack casing, κ_{pack_casing} (W/m K)[b]	0.18	Reaction species initial value electrolyte, $C_{e,0}(1)$[c]	1.00
Emissivity cell surface, $\varepsilon_{cell}(1)$[e]	0.8	Reaction species exponent m SEI, $m_{sei}(1)$[c]	1
Emissivity pack case surface, $\varepsilon_{pack}(1)$[a]	0.5	Reaction species exponent n SEI, $n_{sei}(1)$[c]	0
Convective heat transfer coefficient, h_{conv} (W/m^2 K)	5	Reaction species exponent m NE, $m_{ne}(1)$[c]	1
Heat capacity of air, $C_{p,air}$ (J/kg K)[b]	Eq. (1)	Reaction species exponent n NE, $n_{ne}(1)$[c]	0
Density of air, ρ_{air} (kg/m^3)[b]	Eq. (2)	Reaction species exponent m PE, $m_{pe}(1)$[c]	1
Thermal conductivity of air, κ_{air} (W/m K)[b]	Eq. (3)	Reaction species exponent n PE, $n_{pe}(1)$[c]	1
Activation energy SEI, $E_{a,sei}$ (J/mol)	1.490E05	Reaction species exponent m electrolyte, $m_e(1)$[c]	1
Activation energy NE, $E_{a,ne}$ (J/mol)	1.418E05	Reaction species exponent n electrolyte, $n_e(1)$[c]	0
Activation energy PE, $E_{a,pe}$ (J/mol)	0.963E05	Specific mass of carbon, W_c (kg/m^3)	385
Activation energy electrolyte, $E_{a,e}$ (J/mol)	3.014E05	Specific mass of LFP, W_p (kg/m^3)	615
Frequency factor SEI, A_{sei} (1/s)	1.667E15	Specific mass of electrolyte, W_e (kg/m^3)	510
Frequency factor NE, A_{ne} (1/s)	2.500E13		

[a]Estimated.

[b]*COMSOL Multiphysics 5.2a* built in values [35].

$$C_{p,air} = 1047.63657 - 0.372589265T + 9.45304214 \times 10^{-4}T^2 - 6.02409443 \times 10^{-7}T^3 + 1.2858961 \times 10^{-10}T^4. \quad (1)$$

$$\kappa_{air} = -0.00227583562 + 1.15480022 \times 10^{-4}T - 7.90252856 \times 10^{-8}T^2 + 4.11702505 \times 10^{-11}T^3 + 7.43864331 \times 10^{-15}T^4 \quad (2)$$

$$\rho_{air} = \frac{PM_{dryair}}{RT}, \text{ where } M_{dryair} \text{ (kg/mol) is the molar mass of dry air and } P \text{ (Pa) is the pressure.} \quad (3)$$

[c]Ref. [17].

[d]Ref. [38].

[e]Ref. [15].

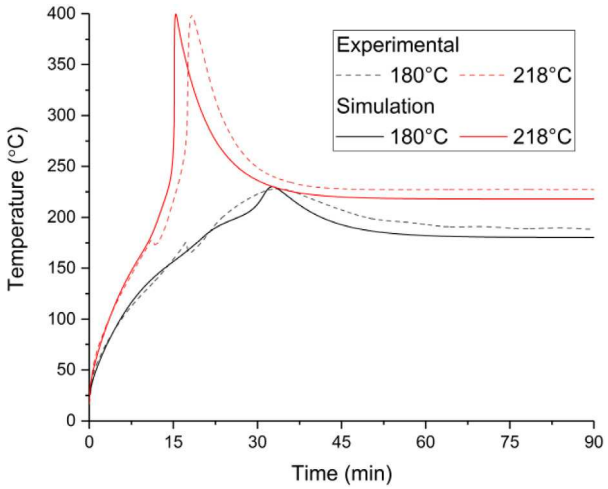

Fig. 3. 2D simulation of a single cell under oven exposure compared to experimental findings. Comparison of cell surface temperatures.

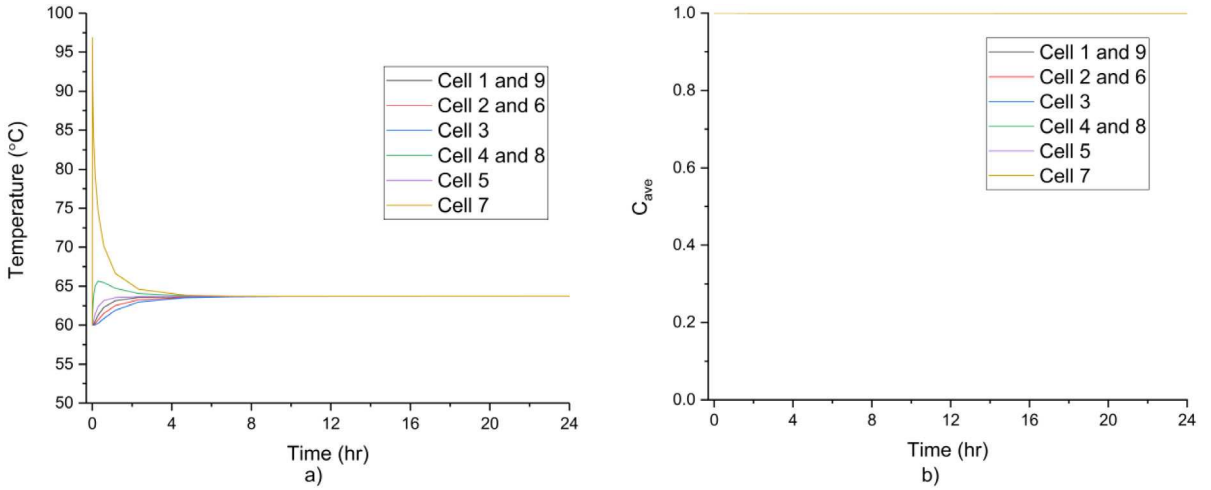

Fig. 4. Abuse of Cell 7 simulating heat released by short circuit, pack under adiabatic conditions. (a) Average cell temperature, (b) average cell decomposition fraction.

2.1. Abuse scenarios of battery pack

The abuse of the battery pack is considered to occur under a worst case scenario, i.e. the pack is initially at a high temperature, 60°C which is representative of the maximum operating temperature of the cell as stated by the manufacture [38], and under adiabatic external boundary conditions. If TRP is predicted under adiabatic conditions then external boundary condition considering convective and radiation heat transfer are also investigated. Two initiation scenarios are considered for the abused cell; (1) a release of 100% of a single cell's electrochemical energy (17.28 kJ) over 10 s representing an external short on the cell, (2) assume an instantaneous temperature rise of 250°C. A corner cell (in this case cell 7) is taken to be the cell abused by an initiation scenario. Again this is to study a worst case scenario, as the literature suggests that the cell in contact with the pack case (environment boundary) and that is also neighbour to the least amount of cells will cause the worst TR event.

3. Results and discussion

3.1. Abuse scenario 1

Fig. 4(a) shows the average cell temperatures against time within the pack when Cell 7 is abuse by an external short and the pack is under adiabatic conditions, while Fig. 4(b) shows the average reaction species of each cell with time. The average reaction species is calculated according to Eq. (4), and is used to allow for clear analysis between multiple cells. Due to symmetry cells 1 and 9, 2 and 6, and 4 and 8 have identical values within their pairs. It can be seen from Fig. 4(a) that TR propagation does not occur. In fact, Fig. 4(b) shows that there is no decomposition present in any cell. Hence, the increase in temperature is purely due to the energy released by the short circuit in Cell 7 and the heat dissipating to the surrounding cells. Fig. 4(b) also shows that the electrochemical energy available in one cell is not enough to increase the abused cells temperature to the point of decomposition reaction onset. Hence, it can be summarized that packs of LFP cells not electrically connected are resilient to TR propagation under the external shorting of a single cell.

$$C_{ave} = \frac{\frac{C_{sei}}{C_{sei,0}} + \frac{C_{ne}}{C_{ne,0}} + \frac{1-C_{pe}}{1-C_{pe,0}} + \frac{C_e}{C_e}}{4} \tag{4}$$

3.2. Abuse scenario 2

Under abuse by an instantaneous temperature rise of 250°C in Cell 7 (to ensure TR occurs in the abused cell) Fig. 5(a) shows that TR throughout the pack does occur when the pack is under adiabatic conditions. Due to the

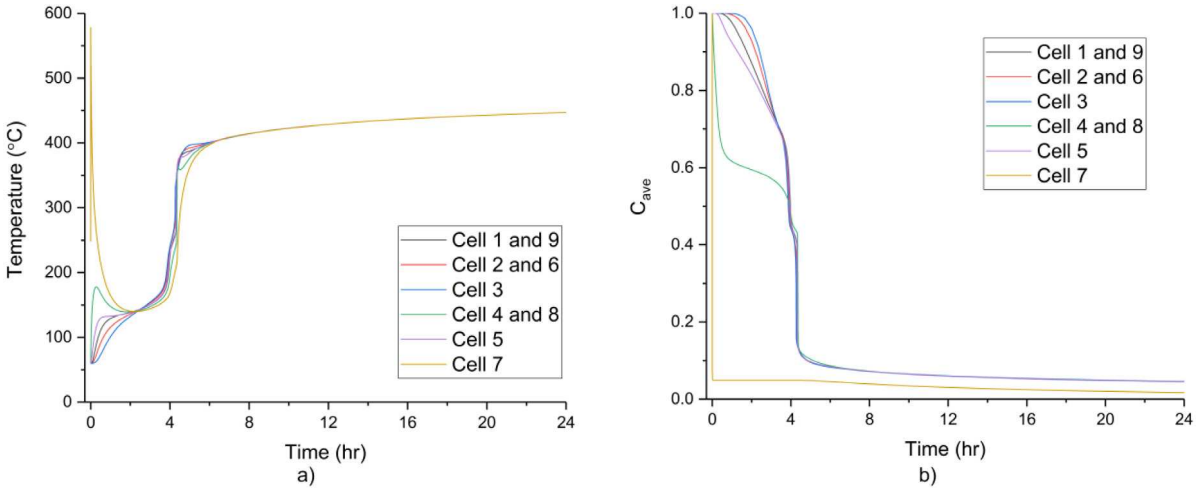

Fig. 5. Abuse of Cell 7 by instantaneous heating to 250°C, pack under adiabatic conditions. (a) Average cell temperature, (b) average cell decomposition fraction.

high initiation temperature of Cell 7, the cell entirely decomposes almost instantaneously, whilst reaching an average temperature of approximately 675°C. Due to the large resulting temperature in Cell 7, leading to large thermal fluxes from the cell, the heat of Cell 7 rapidly disperses to the two cells it is in contact with, i.e. Cells 4 and 8. These cells rapidly decompose by approximately 40% leading to an initial small TR event, after which the cells decompose more slowly as they cool down as heat is lost to the rest of the pack. The remaining cells (i.e. excluding Cells 4, 7 and 8) heat up more slowly, with temperature rates and decomposition rates inversely proportional to their distance from Cell 7.

At approximately 2.5 h the cells within the pack are all equal in temperature, as can be seen from Fig. 5(a), while Fig. 5(b) shows that at 3.5 h all cells excluding 4, 7 and 8 have decomposed by the same degree (i.e. they have the same C_{ave} value), while at 4 h rapid decomposition occurs in Cells 1–3, 5, 6, and 9 almost simultaneously followed by Cell 4 and 8 slightly later. The simultaneous decomposition of Cells 1–6, 8 and 9 is due to the slow behaviour of the decomposition reactions and also their relative stability (i.e. high onset temperature). Hence the heat generated by the decomposition of the cells has the ability to be more evenly dissipated leading to uniform pack temperatures. In this case study, without heat transfer paths through tab connections, this leads to all but the initiation cell to go into TR simultaneously, and not a propagation of cells one after the other going into TR. It should be noted that the time scales leading to TRP are most probably are large over estimate compared to what would occur in a physical pack or if the cell tabs were considered in the model.

Following this, a more realistic scenario is studied, in which the external boundary of the pack considers convection and radiation heat transfer to an extreme environment at 60°C, replacing the former adiabatic boundary condition. The results of this simulation are shown in Fig. 6, where Fig. 6(a) shows the temperature profile and Fig. 6(b) the reaction species profiles. It can be clearly seen from Fig. 6 that TR propagation does not occur. Similarly to the adiabatic case, the high initial temperature in Cell 7 leads to it fully decomposing almost instantly, reaching the same maximum temperature, while Cells 4 and 8 initial decompose rapidly due to the heat transfer from Cell 7, leading to rapid self-heating. However, due to the heat loss from the pack, the initial decomposition (by 15%) of Cells 4 and 8 is less than the adiabatic case as they reach a lower peak temperature than before. Further the remaining cells do not reach a temperature to lead and decomposition of the cells, as seen by the lack of significant change in there average reaction species, hence no TRP.

This shows that even under extreme environmental conditions the heat generated by a single cell under TR is not great enough to lead to TR propagation. This work indicates the potential LFP cells have at providing an inherently safe and abuse resilient technology for large scale batteries.

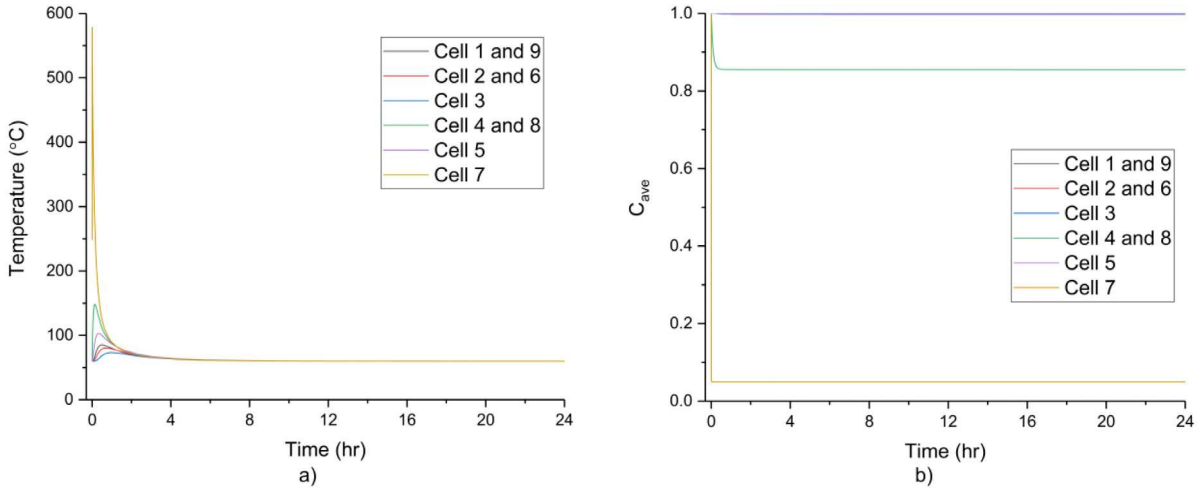

Fig. 6. Abuse of Cell 7 by instantaneous heating to 250°C, pack subject to external environment at 60°C. (a) Average cell temperature, (b) average cell decomposition fraction.

4. Conclusion

A 2D model of an LFP battery pack has been modelled to study its resilience to TRP when one cell in the pack is assumed to undergo a short circuit. It is shown that, when attempting to initiate TR by releasing 100% of a cells electrochemical energy in the shorted cell, the cell does not reach a temperature that leads to cell TR, hence pack TRP does not occur. Under conditions where the shorted cell is forced into TR, by a high initial cell temperature, then the pack goes into TRP if it is under adiabatic conditions. However, when boundary heat transfer is considered, even under extreme external conditions, TRP does not occur. This outlines the potential LFP cells have for facilitating safe and abuse resilient large scale batteries.

Further work is required to validate and improve the predictions of these simulations. This includes extending the model to three-dimension, such that critical heat transfer paths through electrical tab connections can be included, as well as utilizing a more accurate abuse model of a single cell.

Declaration of competing interest

The authors declare that they have no known competing financial interests or personal relationships that could have appeared to influence the work reported in this paper.

Acknowledgements

The authors gratefully acknowledge the financial support of the Engineering and Physical Sciences Research Council (EPSRC), United Kingdom of Great Britain and Northern Ireland in the form of the Energy Storage and its Applications Centre for Doctoral Training (EP/L016818/1).

References

[1] Kim Tae-Hee, Park Jeong-Seok, Chang Sung Kyun, Choi Seungdon, Ryu Ji Heon, Song Hyun-Kon. The current move of lithium ion batteries towards the next phase. Adv. Energy Mater. 2012;2(7):860–72.

[2] Placke Tobias, Kloepsch Richard, Dühnen Simon, Winter Martin. Lithium ion, lithium metal, and alternative rechargeable battery technologies: the odyssey for high energy density. J Solid State Electrochem 2017;21(7):1939–64.

[3] Wang Qingsong, Ping Ping, Zhao Xuejuan, Chu Guanquan, Sun Jinhua, Chen Chunhua. Thermal runaway caused fire and explosion of lithium ion battery. J Power Sources 2012;208(2012):210–24.

[4] Lisbona Diego, Snee Timothy. A review of hazards associated with primary lithium and lithium-ion batteries. Process. Saf. Environ. Protect. 2011;89(6):434–42.

[5] Ohsaki Takahisa, Kishi Takashi, Kuboki Takashi, Takami Norio, Shimura Nao, Sato Yuichi, Sekino Masahiro, Satoh Asako. Overcharge reaction of lithium-ion batteries. J. Power Sour. 2005;146(1–2):97–100.

[6] Lopez Carlos F, Jeevarajan Judith A, Mukherjee Partha P. Experimental analysis of thermal runaway and propagation in lithium-ion battery modules. J Electrochem Soc 2015b;162(9).
[7] Lamb Joshua, Orendorff Christopher J, Steele Leigh Anna M, Spangler Scott W. Failure propagation in multi-cell lithium ion batteries. J Power Sources 2015;283(2015):517–23.
[8] Feng Xuning, Ouyang Minggao, Liu Xiang, Lu Languang, Xia Yong, He Xiangming. Thermal runaway mechanism of lithium ion battery for electric vehicles: A review. Energy Storage Mater. 2018;10(2018):246–67.
[9] MacNeil Dean D, Lu Zhonghua, Chen Zhaohui, Dahn Jeff R. A comparison of the electrode/electrolyte reaction at elevated temperatures for various li-ion battery cathodes. Journal of Power Sources 2002;108(1–2):8–14.
[10] OfWeek. Shenzhen wuzhoulong electric bus burning and explosion, BYD issued an announcement to clarify. 2015, [Online]. Available at: http://nev.ofweek.com/2015-04/ART-71008-8120-28951921.html. (Accessed 19 September 2018). (in Chinese).
[11] Golubkov Andrey W, Fuchs David, Wagner Julian, Wiltsche Helmar, Stangl Christopher, Fauler Gisela, Voitic Gernot, Thaler Alexander, Hacker Viktor. Thermal-runaway experiments on consumer Li-ion batteries with metaloxide and olivin-type cathodes. RSC Adv 2014;4(2014):3633–42.
[12] Jiang Junwei, Dahn Jeff R. ARC studies of the thermal stability of three different cathode materials: $LiCoO_2$; $Li[Ni_{0.1}Co_{0.8}Mn_{0.1}]O_2$; and $LiFePO_4$, in LiPF6 and LiBoB EC/DEC electrolytes. Electrochem Commun 2004;6(1):39–43.
[13] Liu Xuan, Wu Zhibo, Stoliarov Stanislav I, Denlinger Matthew, Masias Alvaro, Snyder Kent. Heat release during thermally-induced failure of a lithium ion battery: Impact of cathode composition. Fire Saf J 2016;85(2016):10–22.
[14] Larsson Fredrik, Anderson Johan, Andersson Petra, Mellander Bengt-Erik. Thermal modelling of cell-to-cell fire propagation and cascading thermal runaway failure effects for lithium-ion battery cells and modules using fire walls. J Electrochem Soc 2016;163(14):A2854–65.
[15] Hatchard TD, MacNeil DD, Dahn JR. Thermal model of cylindrical and prismatic lithium-ion cells. J. Electrochem. Soc. 2001;148(7):A755–61.
[16] Spotnitz Robert M, Franklin James A. Abuse behavior of high-power, lithium- ion cells. J Power Sources 2003;113(1):81–100.
[17] Kim Gi-Heon, Pesaran Ahmad, Spotnitz Robert. A three-dimensional thermal abuse model for lithium-ion cells. J Power Sources 2007;170(2):476–89.
[18] Guo Guifang, Long Bo, Cheng Bo, Zhou Shiqiong, Xu Peng, Cao Binggang. Three-dimensional thermal finite element modelling of lithium-ion battery in thermal abuse application. J Power Sources 2010;195(8):2393–8.
[19] Chiu Kuan-Cheng, Lin Chi-Hao, Yeh Sheng-Fa, Lin Yu-Han, Chen Kuo-Ching. An electrochemical modelling of lithium-ion battery nail penetration. J Power Sources 2014;251(2014):254–63.
[20] Lopez Carlos F, Jeevarajan Judith A, Mukherjee Partha P. Characterization of lithium-ion battery thermal abuse behaviour using experimental and computational analysis. J Electrochem Soc 2015a;162(10):A2163–73.
[21] Peng Peng, Jiang Fangming. Thermal safety of lithium-ion batteries with various cathode materials: A numerical study. Int J Heat Mass Transfer 2016;103(2016):1008–16.
[22] Coman Paul T, Darcy Eric C, Veje Christian T, White Ralph E. Modelling li-ion cell thermal runaway triggered by an internal short circuit device using an efficiency factor and arrhenius formulations. J Electrochem Soc 2017a;164(4):7A58–A593.
[23] Spotnitz Robert M, Weaver James, Yeduvaka Gowri, Doughty DH, Roth EP. Simulation of abuse tolerance of lithium-ion battery packs. J Power Sources 2007;163(2):1080–6.
[24] Yeow Kim F, Teng Ho. Characterizing thermal runaway of lithium-ion cells in a battery system using finite element analysis approach. Int. J. Altern. Powertrains 2013;2(1):179–86.
[25] Kim Gi-Heon, Pesaran Ahmad, Smith Kadler. 2008. Thermal abuse modelling of li-ion cells and propagation in modules. In: The 4th International Symposium on Large Lithium Ion Battery Technology and Application, pp. 1–37.
[26] Kizilel Riza, Sabbah Rami, Robert Selman J, Al-Hallaj Said. An alternative cooling system to enhance the safety of Li-ion battery packs. J Power Sources 2009;194(2):1105–12.
[27] Feng Xuning, He Xiangming, Ouyang Minggao, Lu Languang, Wu Peng, Kulp Christian, Prasser Stefan. Thermal runaway propagation model for designing a safer battery pack with 25Ah $LiNi_xCo_yMn_zO_2$ large format lithium ion battery. Appl Energy 2015;154:74–91.
[28] Liu Xuan, Wu Zhibo, Stoliarov Stanislav I, Denlinger Matthew, Masias Alvaro, Snyder Kent. A thermo-kinetic model of thermally-induced failure of a lithium ion battery: Development, validation and application. J. Electroanal. Soc. 2018;165(11):A2909–18.
[29] Coleman Brittany, Ostanek Jasson, Heinzel John. Reducing cell-to-cell spacing for large-format lithium ion battery modules with aluminium or PCM heat sinks under failure conditions. Appl Energy 2016;180:14–26.
[30] Coman Paul T, Darcy Eric C, Veje Christian T, White Ralph E. Numerical analysis of heat propagation in a battery pack using a novel technology for triggering thermal runaway. Appl Energy 2017b;203(2017):189–200.
[31] Wu Weixiong, Wu Wei, Wang Shuangfeng. Thermal optimization of composite PCM based large-format lithium-ion battery modules under extreme operating conditions. Energy Convers Manage 2017;153:22–33.
[32] Chen Man, Sun Qiujuan, Li Yongqi, Wu Ke, Liu Bangjin, Peng Peng, Wang Qingsong. A thermal runaway simulation on a lithium titanate battery and the battery module. Energies 2015;8(1):490–500.
[33] Xu Jian, Lan Chuanjin, Qiao Yu, Ma Yanbao. Prevent thermal runaway of lithium-ion batteries with minichannel cooling. Appl Therm Eng 2017;110(2017):883–90.
[34] Shack P, Iannello C, Rickman S, Button R. 2014. NASA Perspective and Modeling of Thermal Runaway Propagation Mitigation in Aerospace Batteries. NASA Battery Workshop 2014.
[35] Anon. COMSOL Multiphysics® v. 5.2a. www.comsol.com. COMSOL AB, Stockholm, Sweden.d.
[36] Bugryniec Peter J, Davidson Jonathan N, Brown Solomon F. Assessment of thermal runaway in commercial lithium iron phosphate cells due to overheating in an oven test. Energy Procedia 2018;151(2018):74–8.

[37] Bugryniec Peter J, Davidson Jonathan N, Cumming Denis J, Brown Solomon F. Pursuing safer batteries: Thermal abuse of $LiFePO_4$ cells. J Power Sources 2019;414(2019):557–68.

[38] ENIX Energies. 18650 LiFePO4 Battery 1500mAh 3.2V Data Sheet. 2014, [online] Available at: http://www.enix-energies.co.uk/media/pdf/ACL9011_UK.pdf [Accessed 13 2017].